

## Single-top quark cross-section measurements in ATLAS

DOMINIC HIRSCHBÜHL<sup>1</sup>

ON BEHALF OF THE ATLAS COLLABORATION

*Bergische Universität Wuppertal, 42119 Wuppertal, Germany*

This article presents measurements of all three single top-quark production channels. Detailed measurements of  $t$ -channel single top-quark production using data collected by the ATLAS experiment in proton–proton collisions at a centre-of-mass energy of 8 TeV are shown as well as first results using 13 TeV at the LHC. The associated production of a top quark and a  $W$  boson is presented for data collected at 13 TeV, while the first evidence of single top-quark production in the  $s$ -channel is shown for data collected at 8 TeV.

PRESENTED AT

9<sup>th</sup> International Workshop on Top Quark Physics  
Olomouc, Czech Republic, September 19–23, 2016

---

<sup>1</sup>email: dominic.hirschbuehl@cern.ch

# 1 Introduction

At leading order (LO) in perturbation theory, single top-quark production is described by three subprocesses that are distinguished by the virtuality of the exchanged  $W$  boson. The dominant process is the  $t$ -channel exchange, where a light quark from one of the colliding protons interacts with a  $b$ -quark from another proton by exchanging a virtual  $W$  boson. The total inclusive cross-sections of top-quark and top-antiquark production in the  $t$ -channel in proton–proton  $pp$  collisions at a centre-of-mass energy  $\sqrt{s} = 8$  TeV are predicted to be  $\sigma(tq) = 54.9^{+2.3}_{-1.9}$  pb proton–proton  $pp$  and  $\sigma(\bar{t}q) = 29.7^{+1.7}_{-1.5}$  pb for top-antiquark production and at  $\sqrt{s} = 13$  TeV to be  $\sigma(tq) = 136.0^{+5.4}_{-4.6}$  pb and  $\sigma(\bar{t}q) = 81.0^{+4.1}_{-3.6}$  pb at next-to-leading order (NLO) precision in QCD [1, 2]. The second highest production cross section is predicted for the associated production of a  $W$  boson and a top quark ( $Wt$ ). The cross-section of the  $Wt$  channel at NLO with next-to-next-to-leading logarithmic soft-gluon corrections is calculated as  $\sigma(Wt) = 71.7 \pm 3.8$  pb [3] for  $\sqrt{s} = 13$  TeV. The  $s$ -channel production of a top quark and a  $b$ -quark ( $t\bar{b}$ ) for  $\sqrt{s} = 8$  yields the smallest cross section of  $\sigma(s) = 5.61 \pm 0.22$  pb in NLO QCD [4].

In the following, measurements of all three production channels using data collected by the ATLAS experiment [6] in  $pp$  collisions either at  $\sqrt{s} = 8$  TeV corresponding to an integrated luminosity of  $20.2 \text{ fb}^{-1}$  or  $\sqrt{s} = 13$  TeV at the LHC corresponding to an integrated luminosity of  $3.2 \text{ fb}^{-1}$  are presented.

## 2 $s$ -channel single top-quark production

The analysis for  $s$ -channel single top-quark production is performed using collision data at  $\sqrt{s} = 8$  TeV. Events are selected if they have either of an electron or muon, two jets, where both have to be identified as a jet containing  $b$ -hadrons ( $b$ -tagged jet) and large missing transverse momentum  $E_{\text{T}}^{\text{miss}}$ . After the preselection, the main background are top-quark pair-production ( $t\bar{t}$ ) and  $W$ +jets production. In order to separate the signal from the large background contributions, a matrix element method discriminant is used, see Fig. 1. The signal is extracted from the data utilising a profile likelihood fit, which leads to a measured cross-section of  $\sigma(s) = 4.8 \pm 0.8(\text{stat})^{+1.6}_{-1.3}(\text{syst})$  pb [7]. Dominating uncertainties are Monte Carlo (MC) statistics, jet energy resolution, and the modelling of the  $t$ -channel single top-quark process. The result, which is in agreement with the SM prediction, corresponds to an observed significance of 3.2 standard deviations.

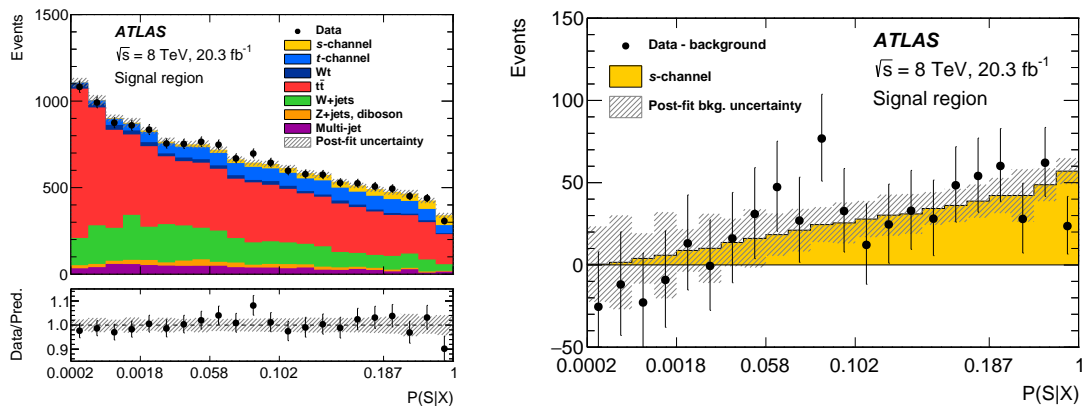


Figure 1: Post-fit distribution of the ME discriminant in the signal region (left). The hatched bands indicate the total uncertainty of the post-fit result including all correlations. Distribution of the ME discriminant in data in the signal region after the subtraction of all backgrounds (right), showing the signal contribution. The error bars indicate the uncertainty of the measurement in each bin [7].

### 3 Associated $Wt$ production

The inclusive cross-section for the associated production of a  $W$  boson and top quark is measured using dilepton events with at least one  $b$ -tagged jet. Events are separated into signal and control regions based on the number of selected jets and  $b$ -tagged jets, and the  $Wt$  signal is separated from the  $t\bar{t}$  background using a boosted decision tree (BDT) discriminant, shown in Fig. 2 The cross-section is extracted by fitting templates to the BDT output distribution, and is measured to be  $\sigma(Wt) = 94 \pm 10(\text{stat})_{-23}^{+28}(\text{syst})$  pb [8]. Main uncertainties are coming from the jet energy scale (JES) and the modelling of the top-quark processes.

### 4 $t$ -channel single top-quark production

The experimental signature of  $t$ -channel single top-quark candidate events is given by one charged lepton (electron or muon), large  $E_T^{\text{miss}}$  and two jets. Exactly one of the two jets is required to be  $b$ -tagged. The main background contributions are the  $t\bar{t}$  and  $W$ +jets processes. In order to separate signal from background an artificial neural network is used, shown in Fig. 3

For the  $\sqrt{s} = 8$  TeV data; the total and fiducial cross-sections are measured for both top quark and top antiquark production. The fiducial cross-section is measured with a precision of 5.8% (top quark) and 7.8% (top antiquark), respectively [9]. A comparison with different MC generator setups is shown in Fig. 4 for the extrapolated

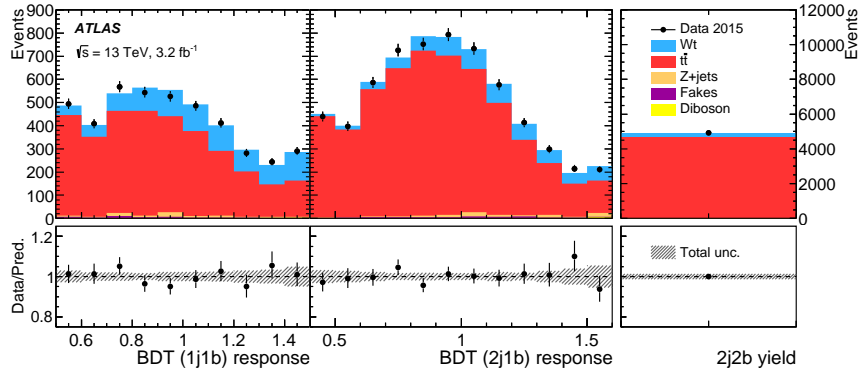


Figure 2: Post-fit distributions of the signal and control regions. The error bands represent the total uncertainties on the fitted results. The upper panels give the yields in number of events per bin, while the lower panels give the ratios of the numbers of observed events to the total prediction in each bin [8].

total cross section. In addition, the cross-section ratio of top-quark to top-antiquark production is measured, resulting in a precise value to compare with predictions,  $R_t = \frac{\sigma_t}{\sigma_{\bar{t}}} = 1.72 \pm 0.09$  and presented in Fig. 5(left). Dominant uncertainties for these measurements are the JES and modelling of the top-quark processes. The total cross-section is used to extract the  $Wtb$  coupling:  $f_{LV} \cdot |V_{tb}| = 1.029 \pm 0.048$ , which corresponds to  $|V_{tb}| > 0.92$  at the 95% confidence level, when assuming  $f_{LV} = 1$  and restricting the range of  $|V_{tb}|$  to the interval  $[0, 1]$ .

Requiring a high value of the neural-network discriminant leads to relatively pure  $t$ -channel samples, which are used to measure differential cross-sections. Differential cross-sections as a function of the transverse momentum and absolute value of the rapidity of the top quark, the top antiquark, as well as the accompanying jet from the  $t$ -channel scattering are measured at particle level and parton level. All measurements are compared to different Monte Carlo predictions as well as to fixed-order QCD calculations where these are available. The SM predictions provide good descriptions of the data.

For the  $\sqrt{s} = 13$  TeV data; the the total cross-sections for both top quark and top antiquark production are measured to be  $\sigma(tq) = 156 \pm 28$  pb and  $\sigma(\bar{t}q) = 91 \pm 19$  pb, respectively [10].

The cross-section ratio is found to be  $R_t = 1.72 \pm 0.20$  and compared with predictions from different PDF groups in Fig. 5 (right). The coupling at the  $Wtb$  vertex is determined to be  $LV \cdot |V_{tb}| = 1.07 \pm 0.09$  and a lower limit on the CKM matrix element is set, giving  $|V_{tb}| > 0.84$  at the 95% CL. These measurements are dominated by systematic uncertainties, from which the uncertainties connected with MC generators are the biggest ones.

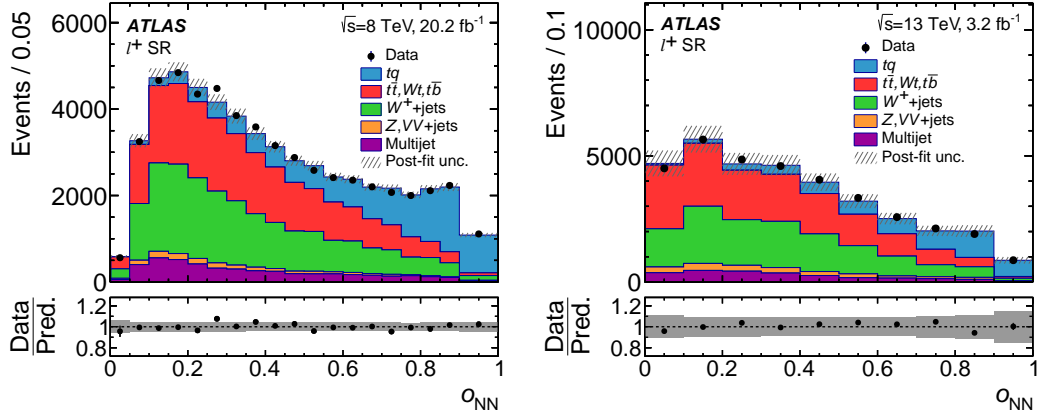


Figure 3: NN discriminant distribution for positively charged leptons in the SR (left) for 8 TeV [9] and (right) for 13 TeV [10]. The signal and backgrounds are normalised to the fit result and the hatched and grey error bands represent the post-fit uncertainty. The ratio of observed to predicted number of events in each bin is shown in the lower histogram.

## References

- [1] J. M. Campbell, R. Frederix, F. Maltoni and F. Tramontano, Phys. Rev. Lett. **102** (2009) 182003
- [2] P. Kant, O. M. Kind, T. Kintscher, T. Lohse, T. Martini, S. Mlbitz, P. Rieck and P. Uwer, Comput. Phys. Commun. **191** (2015) 74
- [3] N. Kidonakis, PoS DIS **2015** (2015) 170
- [4] T. Stelzer, Z. Sullivan and S. Willenbrock, Phys. Rev. D **58** (1998) 094021
- [5] G. Bordes and B. van Eijk, Nucl. Phys. B **435** (1995) 23.
- [6] ATLAS Collaboration, JINST **3** (2008) S08003.
- [7] ATLAS Collaboration, Phys. Lett. B **756** (2016) 228
- [8] ATLAS Collaboration, arXiv:1612.07231 [hep-ex].
- [9] ATLAS Collaboration, arXiv:1702.02859 [hep-ex].
- [10] ATLAS Collaboration, arXiv:1609.03920 [hep-ex].

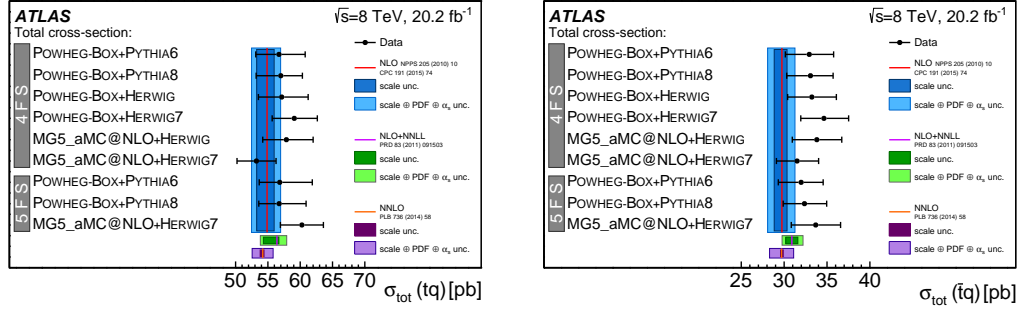


Figure 4: Measured  $t$ -channel single-top-quark and single-top-antiquark fiducial cross-sections compared to predictions by the NLO MC generators POWHEGBOX and MG5\_AMC@NLO in the four-flavour scheme (4FS) and five-flavour scheme (5FS) combined with different parton-shower models (left) for 8 TeV [9] and (right) for 13 TeV [10]. The uncertainties in the predictions include the uncertainty due to the scale choice and the intra-PDF uncertainty.

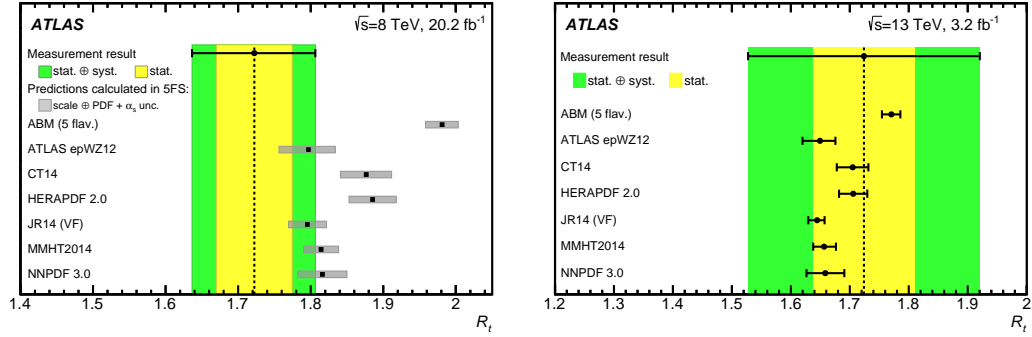


Figure 5: Comparison between observed and predicted values of  $R_t = \frac{\sigma_t}{\sigma_t^{\text{fid}}}$  (left) for 8 TeV [9] and (right) for 13 TeV [10]. Predictions are calculated at NLO precision [1, 2] in the five-flavour scheme and given for different NLO PDF sets. The uncertainty includes the uncertainty in the renormalisation and factorisation scales, as well as the combined internal PDF and  $\alpha_s$  uncertainty. The dotted black line indicates the measured value. The combined statistical and systematic uncertainty of the measurement is shown in green, while the statistical uncertainty is represented by the yellow error band.